

EXAMINATION OF CORE FROM DRILLHOLE OKM3 ON THE WESTERN BANK OF ORAKEI KORAKO GEOTHERMAL FIELD

M.J. Purnomo¹, B.Y. Lynne², S.J. Zarrouk³ and C. Boseley⁴

¹Star Energy Geothermal Indonesia Ltd., Jakarta, Indonesia

²Institute of Earth Science and Engineering, The University of Auckland, New Zealand

³Department of Engineering Science, The University of Auckland, New Zealand

⁴Mighty River Power Ltd., Rotorua, New Zealand

meiyantojp@outlook.com

Keywords: *Orakei Korako alteration, shallow subsurface alteration, Umukuri sinter, Orakei Korako sinter.*

ABSTRACT

The present-day surface activity at Orakei Korako dominantly occurs on the eastern side of the Lake Ohakuri with only minor surface activity on the western bank. A 30 m deep drill hole (OKM3) was drilled on the western bank to monitor the shallow groundwater level. Continuous core was recovered providing the first core from the western side of Lake Ohakuri, as previously reported cored drillholes are located on the eastern side of Lake Ohakuri. Examination of OKM3 core involved identifying the lithology and stratigraphy which consists of pyroclastic rocks of Taupo Pumice alluvium and Akatarewa breccias. At 22 m depth a thin (~10 cm) siliceous sinter horizon is present, indicating historic surface discharge of alkali chloride thermal water.

X-Ray Diffraction (XRD), petrographic microscopy, Scanning Electron Microscopy (SEM) and Energy-Dispersive X-Ray Spectroscopy (EDS) were used to examine hydrothermal alteration within the core. Hydrothermal alteration minerals identified include zeolites (mordenite and clinoptilolite). These zeolites are common alteration products of pyroclastic rocks and infer low temperature alteration (<~100 °C). Zeolite is a late stage alteration product and indicates near-neutral water which may be of meteoric or mixed groundwater and thermal origin. Early stage relict, neutral pH, high temperature, alkali chloride water alteration was identified in the core. Illite-chlorite indicating a series of medium temperature (190-220°C) alteration was identified at 9 to 10 m depth. Illite indicating high temperature (>~220°C) alteration, was identified at 27-28 m depth. The location of the drill site is on an uplifted block of the Emerald fault and this relict alteration indicates temperatures >220 °C where at depth some stage in the past. These findings reveal low temperature hydrothermal alteration has taken place in the shallow environment (<30 m depth) on the western side of Lake Ohakuri. However, historically, high temperature geothermal fluid occurred at depth in this area. Presently, no thermal activity occurs at the surface.

The identification of relict high temperature zone and a previously unknown siliceous sinter horizon at 22 m depth indicates historic flow of alkali chloride fluids at surface and high temperature fluid at depth was more widespread than that of today.

1. INTRODUCTION

In 2011, Mighty River Power Limited (MRP) drilled a shallow well OKM3 to 30 m depth (Fig. 1) to monitor the effect of seasonal and lake level changes to an unconfined

surface aquifer in this field. Core from OKM3 is the first to be recovered from the western bank area at Orakei Korako. The objectives of this study were to document the stratigraphy and alteration assemblages within the core and to assess correlations between cores from OKM3 and core from the eastern bank of the Lake Ohakuri that was documented in 1960s.

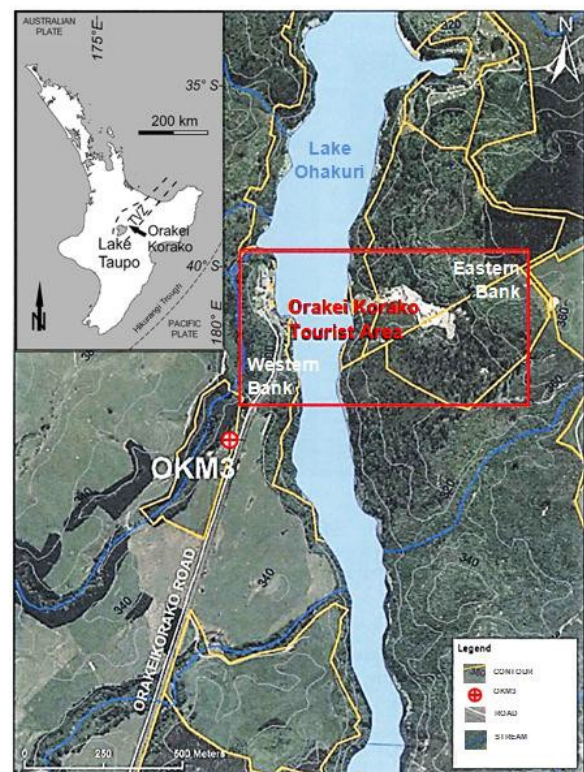


Figure 1: The location of OKM3 well in Orakei Korako (from C. Boseley, personal communication, November 10, 2011).

1.1 Stratigraphy and Structure of Orakei Korako

The stratigraphy of Orakei Korako geothermal field dominantly consists of pyroclastic products overlying Mesozoic greywacke and argillite basement. However, at the surface, the Orakei Korako thermal area only shows the Haparangi rhyolite unit, a pyroclastic and recent deposit which consists of the Waiora formation, Hinuera formation, Taupo Pumice alluvium and expansive sinter terraces (Fig. 2). Structural geology of Orakei Korako geothermal field is mainly controlled by splays of the Paeroa fault, a regional normal fault and also a major fault in the TVZ. This fault is NE-SW trending and down-thrown to the northwest. The

result of the splay is to form the Matangiwaikato fault in the SE and Whakaheke fault in the NW. These faults act as the bounding fault (Lloyd et al., 1972). The region between the two faults is called the Paeroa Fault Zone and consists of parallel faults which have the same trend (NE-SW). For example Golden Fleece, Rainbow, East Wainui and Emerald fault all located at Orakei Korako. The down-throw of these faults is also to the NW direction (Fig. 2).

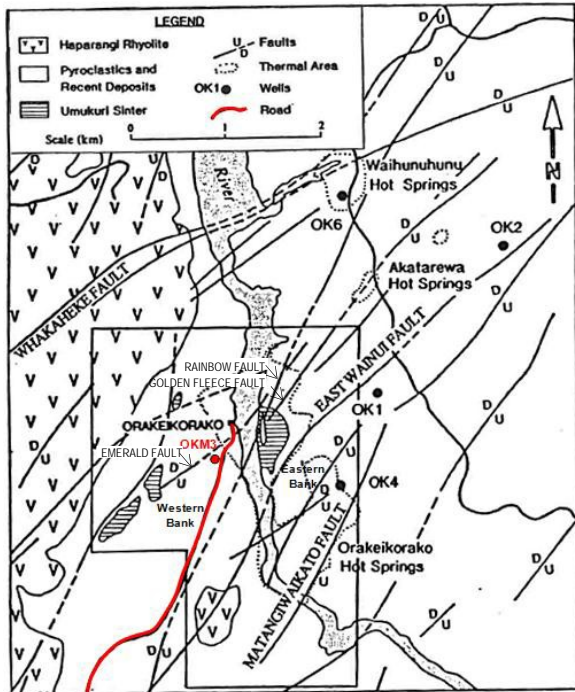


Figure 2: A simplified geology map of Orakei Korako (from Bignall, 1994). The Umukuri sinter is the sinter deposited in the western bank area, while, the silica sinter deposited in the eastern bank is the Orakei Korako sinter (Campbell et al., 2001).

1.2 Geothermal System of Orakei Korako

The Orakei Korako geothermal system is strongly controlled by its structural setting. The thermal manifestations are found in the Paeroa Fault Zone bounded by the Matangiwaikato fault in the SE and Whakaheke fault in the NW. Hydrothermal activity is fault controlled along the bounding faults, steeply dipping intermediate faults and along numerous unnamed faults between East Wainui fault and Matangiwaikato fault (Lloyd et al., 1972 and Hamlin, 1999). Lloyd et al. (1972) suggests that the heat flow from depth can escape to the surface and is controlled by the intersection of NE-SW trending faults with buried N-S trending cross-faults.

Hydrothermal features in this field consist of geysers, pools, mud pools and fumaroles. Orakei Korako consists of two areas: the western bank and eastern bank of Lake Ohakuri. The eastern bank has the most prominent hydrothermal features including numerous hot springs and an area of 1.3 km² of warm ground (Bignall, 1994). The hydrothermal manifestations are concentrated close to the river (now drowned), and others are located at the foot of the recent fault and at a higher elevation. The recent fault is acting as a channel for the flow of hot water (70-90°C) to the surface and where it has deposited extensive silica sinter terraces. All the springs and geysers are discharging near neutral pH (7.5-9), alkali chloride-bicarbonate water, with low salinity.

Meanwhile, in the western bank most of the manifestations are located adjacent to the river or are drowned under Lake Ohakuri.

1.3 Previous Hydrothermal Alteration Studies of Orakei Korako

The surface alteration in this geothermal field is an advanced argillic - argillic alteration. These types of alteration consist mainly of kaolin group product of neutral pH, mixed alkali chloride-bicarbonate fluid which is superseded by steaming ground (Bignall, 1994).

The shallow subsurface (120 m depth) alteration minerals based on the core from a drillhole on the eastern bank, as discussed by Hamlin (1999), consisted of calcite, chlorite, kaolinite, illite, smectite, interlayer illite-smectite and zeolite (clinoptilolite, mordenite and stilbite). The shallow subsurface alteration shows two distinctive periods, (1) high temperature fluids and (2) low temperature fluids. The alteration from the high temperature time (> 220°C) was produced by alkali-chloride water and was overprinted by lower temperature (180-220°C) alteration. Some of the high temperature minerals were observed at shallow depth (30-50 m depth). The occurrence of illite in near surface zones is interpreted as resulting from one of several possible causes as given below (Hamlin, 1999): (1) Relict alteration product which was brought to the shallow subsurface by faulting, (2) Illite might have formed at temperatures < 220°C, (3) The source of illite was detritus of eruption breccia from depth and not hydrothermal alteration (4) Fluid with temperatures above 220°C flowed at that depth. Hamlin (1999) suggested that option three and four might control the presence of illite at shallow depths. The lowest temperature alteration assemblage was from alkali-chloride water at <120°C proven by the occurrence of zeolite (mordenite + clinoptilolite). This alteration may be caused by mixing of alkali-chloride water with surface water and reactions with the host rock. The presences of steam-water reactions are indicated by kaolinite. Kaolinite which occurs together with zeolite (mordenite + clinoptilolite) in this well indicates a change of fluid from acid to alkali.

The deep mineral assemblage (below 500 m depth) from core of a drillhole in the eastern bank shows quartz-adularia zones occur. This mineral assemblage indicates temperatures in the range of 210-300°C. The distribution shows shallow upwelling thermal fluid in the OK4 area with a cooler flow (outflow) to the OK6 area (roughly south to north direction). The centre of upwelling itself was located at the OK2X area. There is evidence that cooling events happened in this field, especially in the southern part (OK4). These cooling events were also reflected in fluid inclusion analysis. The Tbore (direct temperature measurement in the hole) in OK4 shows a maximum of 238°C (Bignall, 1994). However, The Th (homogenisation temperature) of fluid inclusions show a maximum of 312°C (Bignall, 1994). The centre of the system seems to have migrated to the northern part of the field. Fluid inclusion and mineral temperatures show a heating process has taken place in that area. For example, at OK6 (1113.4 m depth), Tbore shows maximum temperature of 261°C. However, Th only shows a maximum temperature of 210-221°C (Bignall, 1994).

2. METHODS

Core from OKM3 was described in terms of its lithology and alteration. Further examination involved thin section analysis from selected samples representing each lithology

and stratigraphic unit. XRD whole rock (bulk) analysis parameters (for powder size $>2\mu\text{m}$) were applied to 21 samples mounted on an aluminium holder to determine the minerals within the samples. XRD operating conditions were 2° to 45° for 20 with a step size of 0.02° at a speed of $1.05^\circ/\text{minute}$. Clay mount analysis (for powder size $<2\mu\text{m}$) was applied to 18 samples. XRD operating conditions for clay analysis was 2° to 32° for 20, with a step size of 0.03° at $1.05^\circ/\text{minute}$. Determination of the clay attributes follows the method given by Moore & Reynolds (1989). The method is based on the R-value (Reichweite value) which is derived from the value of 001/002 and 002/003 illite peak in interstratified clay. The R-value is used to estimate the percentage of illite in the interstratified clay. The R-value is also used to estimate the formation temperature based on methods by Jennings & Thompson (as cited in Harvey & Browne, 1991). XRD SiO_2 sinter analysis (for powder size $>2\mu\text{m}$) was applied to 3 samples. This analysis was used to determine the silica phase of the samples. The XRD operating conditions were 10° to 40° for 20 with a step size of 0.01° at $0.6^\circ/\text{minute}$. The FWHM (Full Width at Half Maximum) value of the sinter samples is calculated from the diffraction band and indicates the silica phase and degree of silica phase maturation. The operating conditions used for XRD and the FWHM analysis is based on methods by Herdianita et al., (2000) and Lynne et al., (2007). Scanning Electron Microscopy (SEM) analysis was used to examine the morphological characteristics of silica samples (clast and layer) and mineral growth. Two samples representing the silica zone were examined. Electron Dispersive Spectroscopy (EDS) was used to determined the chemical composition of specific areas within the samples of mineral growth

3. RESULTS

3.1 Cored Rocks Description

Core rock descriptions show various types of pyroclastic rocks (lapilli tuff, lapilli stone, tuff and lapilli-tuff breccia). In general, the most common lithology was lapilli tuff (Fig. 3.a). The silica clast and a silica layer were found in this lithologic unit at 22 m depth (Fig. 3.b). The rock with the silica layer, 10 cm thickness, has a poorly sorted texture with the groundmass consisting of a fine grain size, although some segments show a fine to coarse grain size as well. Coarse ash layers and thin bedded structures were found as well in this lapilli tuff. In general, this lapilli tuff indicates normal grading. However, symmetric grading (normal to reverse) and reverse grading was observed in some locations. Lapilli stone (Fig. 3.c) occurs in the shallow part of OKM3, in between lapilli tuff units (8-12 m depth). Lapilli consist of pumice and crystal fragments with a minor lithic component. Silica clasts are rarely found. This lapilli stone have various deposition textures. A poorly sorted texture occurs while some parts show a medium sorted bedded structure (thin bedded structure). Symmetric grading (normal to reserve) is found in this unit. Tuff (Fig. 3.d) occurs in minor quantities between lapilli tuff units (17-18 m depth) with minor coarse ash nodules. The nodules consist of minor crystal and lithic fragments. Lapilli-tuff breccia (Fig. 3.e) occurs in the deeper part of the well (24-29 m depth). The composition consists of pumice and crystal lapilli. The groundmass is composed of fine volcanic ash. Vesicles are common in this unit and it shows a growth of minerals (Fig. 3.e). The texture of this unit indicates poorly sorted deposition. The groundmass displays flattening and flowing-like structures which may indicate evidence of a welding process.

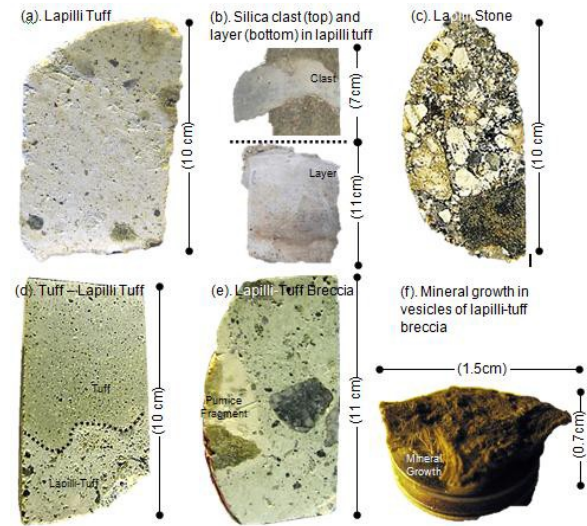


Figure 3: Representative core samples showing the various lithologic units.

Classification of the alteration of the core samples is based on color and changes of the lithology properties (e.g., texture, hardness and density). In general, alteration in this core consists of kaolinite and zeolite. However, some parts of the core display a denser zone which may indicate a siliceous cementing process. Kaolinite alteration is characterized by changes of ash in the groundmass from light grey to white and light yellow, soft and chalky material (Fig. 4.a). This type of alteration occurs in the shallow part of the well (from near surface down to 12 m depth). Zeolite alteration is mainly characterized by soft and pale green to green rock containing clayish material (Fig. 4.b) and occurs in the shallow part (6 m depth) to the bottom of the well (30 m depth). The silica cementing process is found associated with kaolinite and zeolite alteration.

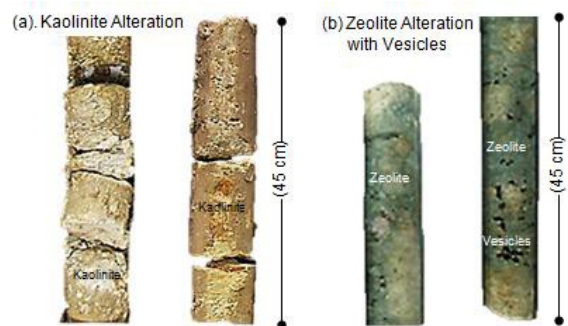


Figure 4: The type of alteration observed from the core samples.

Alteration intensity cannot be clearly defined. However, based on the level of changes of rock properties, the alteration may show weak to moderate intensity. The alteration shows no correlation with fractures in this core. The fractures dominantly have 60° apparent dip and a narrow opening. Traces of a weathering process in the form of an oxidation zone are indicated. No veins occur in this core. Therefore, the alteration process in this core is controlled by primary permeability (e.g., pore spaces between fragments or pore spaces in the groundmass and fragments).

3.2 Petrographic Microscopy

Pumiceous-lithic tuff, vitric tuff and vitric-crystal tuff were identified using petrographic microscopy. The pumiceous-lithic tuff (Fig. 5.a), was the most common unit identified in six samples and displayed a poorly sorted texture. Most of the samples indicate a dense rock. However, some samples demonstrate a more porous rock (intergranular porosity) (Fig. 5.b). A continuous flow-like structure displaying folding of glass shards surrounding the crystals occurs at 26 and 28 m depth. However, this structure did not create a flattening of pumice fragments (fiamme structure) or the alignment of elongated crystals and lithic fragments. Even though the Y-shape of the glass and the bubble walls in the glass had collapsed. Therefore, this structure does not demonstrate a well-developed welded tuff (How Volcanoes Work, 2013).

Vitric tuff (Fig. 5.c) was identified in three samples and consists of pumice and quartz crystals. A poorly sorted texture is clearly visible in thin section (Fig. 5.c). Groundmass is dominant and creates a denser rock.

Vitric-crystal tuff (Fig. 5.d) was identified in one sample. The dominant fragment composition is quartz, with some lithic and pumice fragments. The groundmass is dominated by volcanic ash making this rock dense. It is poorly sorted.

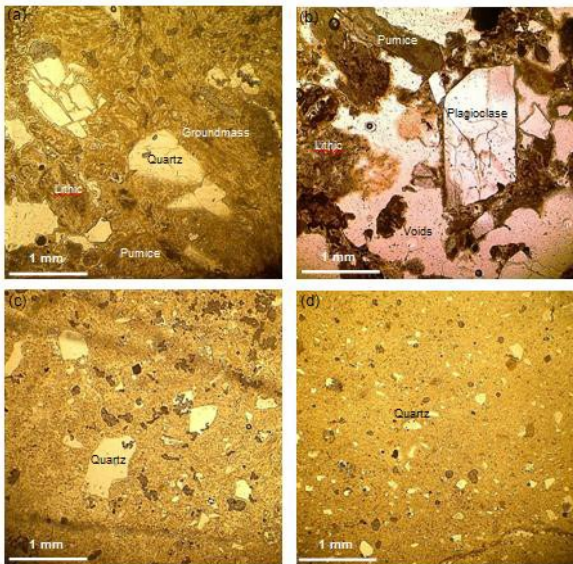


Figure 5: Photomicrographs of thin sections from core OKM3. (a) A dense pumiceous lithic tuff. (b) The porous pumiceous lithic tuff. (c) Vitric tuff with poorly sorted texture. (d) A dense vitric-crystal tuff.

Based on this analysis the hydrothermal alteration of this core can be divided into two types (1) clay minerals and (2) zeolite minerals. Clay minerals occurred in the form of kaolin, smectite, illite or chlorite, which was also determined by XRD analysis. Clay minerals in the shallow part of OKM3 (up to 8 m depth) show minor distribution of pumice, plagioclase and lithic fragments. These clay minerals also occur in the groundmass, although their distribution is minor. The amount of clay minerals increased at 22 m depth, and is mainly distributed in the groundmass, even though minor clay minerals occurred in pumice and plagioclase crystals. The most abundant clay minerals occur at 24 m depth where there is intensive clay

mineral deposition in pore spaces between fragments (Fig. 6.a). These clay minerals also occur in pumice, plagioclase and replace biotite. Below 24 m depth, the occurrence of clay minerals decreases with depth. Clay minerals occur in the groundmass below 26 m depth. The clays are distributed between fragments and around opaque minerals. At this depth, these clay minerals occur as replacements for plagioclase and biotite fragments. At the bottom of the well (30 m), minor clay minerals occur in the groundmass.

Other hydrothermal minerals occurring in the samples are zeolites. The most prominent zeolite mineral is heulandite/clinoptilolite which is present in most samples. Heulandite/clinoptilolite is deposited in voids of glass shards which show up as typical prism crystals (Fig. 6.b). Another zeolite mineral is mordenite which is characterized by needle shaped crystals. Mordenite also typically occurs in voids of glass shards (Henneberger and Brown, 1988). Mordenite distribution is mainly in the deep part of the well (26 m depth).

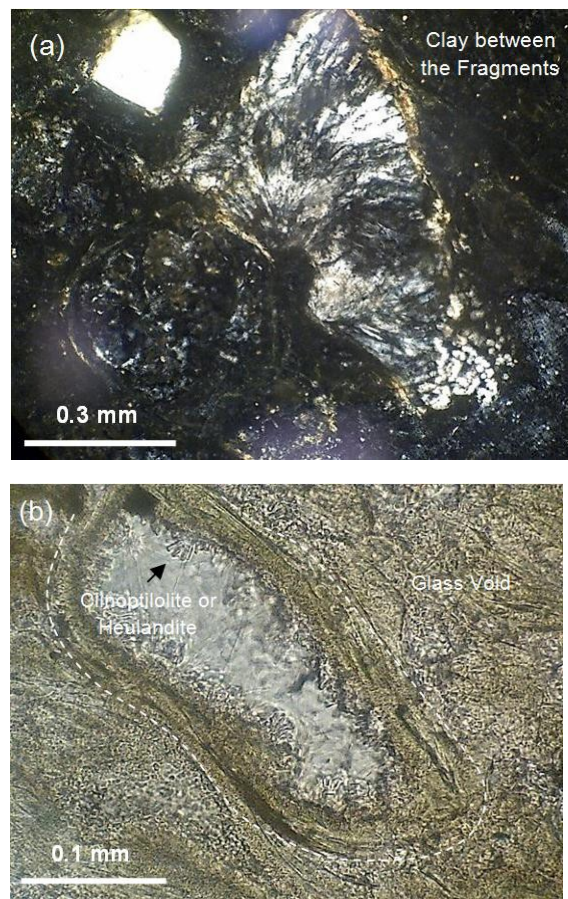


Figure 6: (a) The clay mineral distribution in pore spaces between fragments observed from thin section analysis. (b) Mordenite identified in a glass void.

The secondary silica minerals were found in almost all samples as well as clay minerals. The distribution of secondary silica is mainly in the groundmass. Small amount of secondary silica occurs in the fragments. The distribution of silica varies with depth. Samples from near the surface (14 m depth) have silica distributed in the groundmass and the fragments. The silica decreases below this 14 m depth. At 22 m depth, the silica occurs in the groundmass and fragments. Below this depth, the silica is mainly found in

the groundmass and concentrated in voids between fragments. This silica mineral may be the result of zeolite alteration which replaces ash and pumice in the rocks to secondary silica minerals.

3.3 XRD Analysis

The XRD result confirms that the clay minerals observed in the samples consist of kaolinite (metahallosite + kaolinite-smectite) and smectite above 9 m depth. The interlayered illite-smectite, illite-chlorite and illite were observed below 9 m depth. Zeolites were found in most of the core. The common zeolite minerals occurring in core OKM3 are clinoptilolite and stilbite with minor amounts of mordenite and laumontite. Further analyses of the interstratified clay, especially kaolinite-smectite and illite-smectite, showed the percentage composition of clay and were used to infer the formation temperature. The composition of kaolinite in the kaolinite-smectite layer is around 80-90%, and the smectite displays only 10-20%. This result indicates kaolinite is more dominant in the interstratified kaolinite-smectite in OKM3 core. The composition of illite-smectite based on the same method shows the percentage of illite varies from 40-50%. Therefore, smectite clay is dominant in this core. The R-value based on this composition is zero (0). This value indicates the temperature of crystallization to be below 130°C.

The silica phase from the XRD analysis for the silica layer and silica clasts consists of opal-CT and quartz. Silica clasts located above 22 m depth consisted of opal-CT with a FWHM value of 0.46° for 20. The silica layer at 22 m depth consists of opal-CT with minor quartz and a FWHM value of 0.67° for 20, while the silica clast at 24 m depth consists of opal-CT and quartz with a FWHM value of 0.46 ° for 20.

3.4. SEM/EDS ANALYSIS

SEM was performed on samples from the silica deposition zone and on the silica clasts. The SEM results from the silica clast show that it consists of opal-CT. The opal-CT displays sharply bladed lepispheres (Fig. 7.a). However, some lepispheres indicated an early stage of opal-CT formation shown by the more rounded bladed morphology (Fig. 7.b). The less bladed lepispheres consist of aligned nanospheres which demonstrate late opal-A/CT, a precursor silica phase to opal-CT. XRD analysis of the silica layers shows the silica phase to be opal-CT. However, SEM observations show opal-CT lepispheres are dominated by aligned nanospheres, which indicate the morphology to be opal-A/CT (Fig. 7.c).

The occurrence of plant molds is abundant in the silica layer sample (Fig. 7.d). The plant mold is characterized by circular and elongated tubes. Some molds are lined with opal-A/CT. This plant mold suggests that this silica layer is part of more extensive silica sinter deposit. Plant molds are common in sinters from numerous geothermal fields (Lynne, 2013) and are characteristic of low temperature (<35 °C) alkali chloride water.

SEM images show details of mineral growth in vesicles at 27-28 m depth. This mineral growth displays a crystalline and plate-like structure (Fig. 8) which can be observed in the core samples. The other mineral has a fibrous structure and entombs the plate-like structured mineral (Fig. 8). To determine the elemental composition of the minerals, Energy-Dispersive Spectroscopy (EDS) was used. EDS showed both minerals are composed of O, Al, Si, K and Ca indicating zeolite minerals. For the crystalline, plate-like

structure mineral, based on the ratio between Al and Si which displays ≥ 4 (4.52) and considering their morphology, the zeolite is clinoptilolite (Coombs et al., 1997 and Welton, 1984). The other zeolite mineral which has a fibrous structure is mordenite (Welton, 1984) (Fig. 8).

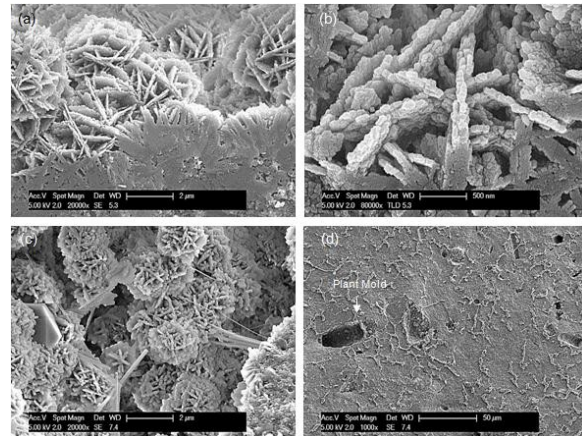


Figure 7: (a) SEM images of a silica clast at depth 21.8-22 m depth reveals opal-CT silica. (b) The less bladed morphology of opal-A/CT. (c) SEM images of a silica layer at depth 22 m depth reveals opal-A/CT. (d) Plant molds observed in the silica layer at 22 m depth.

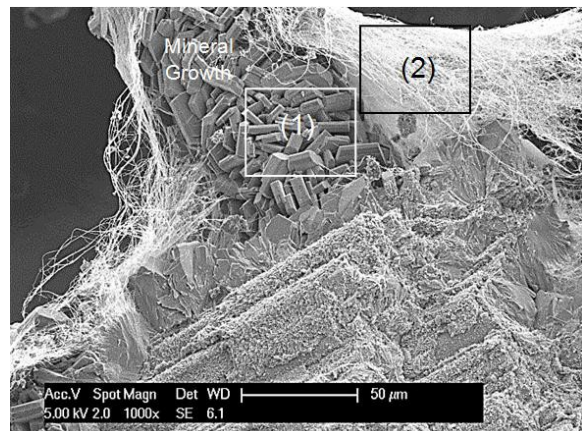


Figure 8: The SEM scans of mineral growth in vesicles display crystalline and plate-like structure minerals (1). Minerals displaying a fibrous structure entomb platy structure minerals (2). The location of EDS scans of mineral growth in vesicles indicated a zeolite mineral of clinoptilolite at square (1) and mordenite at square (2).

4. DISCUSSION

4.1 Lithology and Stratigraphy

The lithology of OKM3 clearly indicates pyroclastic rocks dominate the core. These pyroclastic rocks consist of Lapilli Tuff, Tuff, Lapilli-Stone and Lapilli-Tuff Breccia and are composed of Pumiceous-Lithic Tuff, Vitric Tuff and Vitric-Crystal Tuff. A unique siliceous sinter layer, 10 cm thick, is present at 22 m depth. SEM observations show the sinter layer consists of late stage opal-A/CT to early opal-CT. However, the XRD result indicates a more advanced silica phase of opal-CT. Lynne and Campbell (2004) determined that silica phase changes in mineralogy

can precede the morphological transitions. Plant molds preserved within this sinter layer suggest a marginal depositional low-temperature setting ($<35^{\circ}\text{C}$) (Lynne, 2013). Dating of the sinter is required to determine its age, which was outside the scope of this study. Dating would determine if the discharging alkali chloride fluids at OKM3 were concurrent with those discharging at the nearby Umukuri sinter located 0.5 km to the SE of OKM3 or whether it formed at the same time as historic sinters located 0.5 km away on the eastern bank of Orakei Korako. The origin of the silica clast which does not have the characteristics of sinter is possibly a volcanic tuff.

Based on the comparison with the known stratigraphy of Orakei Korako by Lloyd et al., (1972) and Bignall (1994), the Lapilli-Tuff breccia identified below the siliceous sinter deposit may be part of the Akatarewa breccia. In this core, the unit deposited above the siliceous sinter layer is Taupo Pumice alluvium. The thin bedding of coarse and fine ash indicates periods of pyroclastic fall (air fall ash) dominated the depositional processes.

4.2 Hydrothermal Alteration

Three groups of mineral assemblage were identified in this study. The first mineral assemblage consists of advance argillic alteration which consists of the kaolinite group. This mineral assemblage indicates the dominant fluid type controlling the alteration is acid sulphate which is a result of oxidation of steam heated water. The kaolinite zone occurs above 9 m depth in OKM3.

The second mineral assemblage is argillic which consist of zeolite, smectite and interlayer illite-smectite. This zeolite alteration assemblage is usually associated with meteoric water. Henneberger and Brown (1988) identified a group of zeolites consisting of clinoptilolite and mordenite at the Ohakuri geothermal system (± 9 km NNW of Orakei Korako), resulting from alteration by mixed chloride-water and groundwater. In OKM3 the zeolite assemblage occurs throughout the well. Therefore, a period of alteration dominated by meteoric water or mixed chloride-water and groundwater takes place in the upper 30 m at the site of OKM3. The group of zeolite minerals, at Ohakuri, is associated with silica (predominantly opal-CT). Hence, the secondary silica mineral found in the pumice fragments and groundmass in this well may be part of this alteration group. Smectite occurs in the near surface zone (6 m depth). It is usually associated with bicarbonate water or mixed chloride water and acid sulphate water (Hedenquist as cited in Bignall, 1994). Interlayer illite-smectite indicates bicarbonate water dominates (Hedenquist as cited in Bignall, 1994). Illite-smectite occurs at the near surface (10 m depth) and in deeper parts of the core (22 m depth).

The third mineral assemblage is propylitic which consists of illite-chlorite and illite. These minerals result from alteration by neutral pH alkali-chloride water (Hedenquist as cited in Bignall, 1994). Illite-chlorite occurs in the upper section of the core (9-10 m depth) and in the deeper part (26 m depth). Illite occurs at 27-28 m depth.

Temperature regimes in this well can be inferred from the mineral assemblages. Advanced argillic which consist of kaolinite shows a range of temperature between $100-130^{\circ}\text{C}$ (Hedenquist as cited in Bignall, 1994). Henneberger and Brown (1988) stated the kaolinite indicates temperatures $<100^{\circ}\text{C}$. Brown (1978) stated that kaolinite may not persist above 60°C . Therefore, the temperature of this zone in this

well may indicate temperatures of $< 130^{\circ}\text{C}$. Zeolite minerals, especially clinoptilolite and mordenite infer temperatures of $< 100^{\circ}\text{C}$ (Henneberger and Brown, 1988). Smectite which is part of argillic mineral assemblage has a formation temperature of $\sim 70^{\circ}\text{C}$ (Harvey and Browne, 1991). Interlayered illite-smectite in OKM3 is also part of the argillic mineral assemblage and indicates a higher temperature range of $100-150^{\circ}\text{C}$. Nevertheless, the temperature inferred from the R-values of the interlayered illite-smectite shows a range of temperatures $< 130^{\circ}\text{C}$. Interlayer illite-chlorite is part of propylitic mineral assemblages and has formation temperatures of $190-220^{\circ}\text{C}$ (Harvey and Browne, 1991). Illite which is also part of this group shows a range of temperatures $> 220^{\circ}\text{C}$ (Harvey and Browne, 1991 and Browne as cited in Hamlin, 1999).

The fluid and thermal history can be summarized from the inferred fluid type and temperature. In general, the mineral assemblages indicate an early stage historic neutral pH alkali-chloride fluid temperature $190-220^{\circ}\text{C}$ in the near surface of OKM3 (9-10 m depth) and other fluid with temperature $> 220^{\circ}\text{C}$ in the deeper part (27-28 m depth). During the cooling process, steam escapes from this fluid, which condensed in non-oxygenated groundwater, creating zones of low temperature bicarbonate water ($<130^{\circ}\text{C}$) above and below the hot fluid zone (Hedenquist as cited in Bignall, 1994). Alternatively, steam in the near surface (above 9 m depth) condensed in the groundwater and oxidized, creating a zone of acid sulphate water ($<130^{\circ}\text{C}$). This late stage was dominated by the mineral assemblage indicating surface water or mixing between alkali-chloride water with groundwater at temperatures $< 100^{\circ}\text{C}$. This is evident throughout the core.

Intensity of alteration involved high temperature neutral pH alkali-chloride water based on the occurrences and distribution of the clay minerals. The most intense alteration happens in the porous rocks. Intensity alteration may be inferred from the zeolite alteration minerals. Henneberger and Brown (1988) stated that clinoptilolite indicated less intense alteration compared to mordenite in the Ohakuri geothermal field. Therefore, the zeolite alteration is more intensive in the deeper part (below 26 m depth) of OKM3.

Correlation between the alteration of OKM3 with work by Hamlin (1999) suggests that the same high temperature mineral assemblages (located at < 30 m depth at OKM3) occur within cores from the shallow part (30-50 m depth) of drill holes OK1 and OK2X located on the eastern bank of Orakei Korako. OK1 is located at the up-thrown side of the East Wainui fault and OKM3 is located on the upthrown side of Emerald fault. These fault structures provide permeable channels for fluids to flow and discharge at the surface. The shallow depths of the high temperature mineral assemblages on the up-thrown side of major faults in the area suggest these blocks have been uplifted to shallow depth. Uplifted high temperature mineral assemblages are documented by Bignall and Browne (1994) at Te Kopia along the fault scarp. All the high temperature ($> 220^{\circ}\text{C}$) alteration zones in OK1, OK2X and OKM3 have been overprinted by lower temperature alteration minerals (zeolite alteration) indicating a decrease in temperatures to $< 100^{\circ}\text{C}$ in the area.

5. CONCLUSION

Well OKM3 is a shallow well (30 m depth) drilled on the western bank of the Lake Ohakuri at the Orakei Korako

geothermal field. OKM3 is the only well drilled on the western bank. The lithology and stratigraphy of the well consists of pyroclastic rocks, with Taupo Volcanic alluvium in the upper part (near surface – 22 m depth). A thin siliceous sinter layer was found at a depth of 22 - 22.1 m. Plant molds in the sinter infer it was located a significant distance from the vent and deposited from low temperature discharging fluids (<35 °C) (Lynne, 2013). Below this sinter (22.1 - 30 m depth), the stratigraphy consists of pyroclastic products of the Akatarewa breccia. This breccia is part of Waiora formation.

The hydrothermal alteration shows several temperature regimes and fluid types. In general, two types of hydrothermal fluid and temperature regimes are present in OKM3 core. An early stage, high temperature (190-220°C and >220°C) neutral pH alkali chloride water, alteration zones are observed at 9-10 m and 27-28 m depth. However, it is unlikely that high temperature mineral assemblages occurred at such shallow depths. It is more likely that the alteration took place at a greater depth with fault activity uplifting the high alteration mineral zone to a shallow depth. The second alteration is a late stage alteration, mainly involving surface water or a mixture of alkali-chloride water with groundwater in low temperature conditions (<100°C) to produce a zeolite alteration zone. Based on similarities with zeolite alteration described by Henneberger and Brown (1988) in the Ohakuri geothermal field, the late stage alteration at OKM3 represents a marginal part of the geothermal system. Hence, OKM3 well has experienced a change from high temperature neutral pH alkali-chloride water to a low temperature marginal area alteration.

Correlation with cores from the eastern part of Orakei Korako shows high temperature (> 220°C) activity occurred at the same depth. This activity may be controlled by high permeability zones associated with faults. OK1, OK2X and OKM3 drill holes are located close to the East Wainui and Emerald fault. Therefore, these faults might act as conduits for reservoir fluid to flow to the near surface. Also OK1 and OKM3 wells are located on the up-thrown part of East Wainui and Emerald faults. Uplift along the faults would bring the relict high temperature alteration zone to shallower depths. Erosion following uplift could further expose rocks from depth in the near the surface.

ACKNOWLEDGEMENTS

The authors would like to thank Mighty River Power Ltd. for permission to use the data discussed in the paper and to acknowledge the help provided by Novi Ganefianto (MRP), Andrew Rae (GNS) and Patrick R.L. Browne (IESE).

REFERENCES

Bignall, G., & Browne, P. (1994). Surface Hydrothermal Alteration and Evolution of the Te Kopia Thermal Area, New Zealand. *Geothermics*, 23(5), 645-658.

Bignall, G. (1994). Thermal Evolution and Fluid-Rock Interactions in the Orakeikorako-Te Kopia Geothermal System, Taupo Volcanic Zone, New Zealand (Doctoral Dissertation, ResearchSpace@Auckland).

Browne, P. (1978). Hydrothermal Alteration in Active Geothermal Fields. *Annual Review of Earth and Planetary Sciences*, 6, 229-250.

Campbell, K. A., Sannazzaro, K., Rodgers, K., Herdianita, N., & Browne, P. (2001). Sedimentary Facies and Mineralogy of the Late Pleistocene Umukuri Silica Sinter, Taupo Volcanic Zone, New Zealand. *Journal of Sedimentary Research*, 71(5), 727-746.

Coombs, D. S., Alberti, A., Armbruster, T., Artioli, G., Colella, C., Galli, E., Minato, H. (1998). Recommended Nomenclature for Zeolite Minerals; Report of the Subcommittee on Zeolites of the International Mineralogical Association, Commission on New Minerals and Mineral Names. *European Journal of Mineralogy*, 10(5), 1037-1081.

Hamlin, K. A. (1999). Geological Studies of the Orakeikorako Geothermal Field, Taupo Volcanic Zone / Kirsty A. Hamlin. Thesis (MSc--Geology)--University of Auckland, 1999.

Harvey, C. C., & Browne, P. R. (1991). Mixed-Layer Clay Geothermometry in the Wairakei Geothermal Field, New Zealand. *Clays and Clay Minerals*, 39(6), 614-621.

Henneberger, R., & Browne, P. (1988). Hydrothermal Alteration and Evolution of the Ohakuri Hydrothermal System, Taupo Volcanic Zone, New Zealand. *Journal of Volcanology and Geothermal Research*, 34(3), 211-231.

Herdianita, N., Browne, P., Rodgers, K., & Campbell, K. (2000). Mineralogical and Textural Changes Accompanying Ageing of Silica Sinter. *Mineralium Deposita*, 35(1), 48-62.

How Volcanoes Work - Microscope Ignimbrite Textures Retrieved 5/22/2013, 2013, from http://www.geology.sdsu.edu/how_volcanoes_work/ignimbrite_textures.html

Lloyd, E. F., Mahon, W. A. J., & Boielle, L. (1972). Geology and Hot Springs of Orakeikorako. New Zealand, Department of Scientific and Industrial Research.

Lynne, B. Y. (2013). Siliceous Sinter an Early Exploration Tool and Direct Link to a Geothermal Reservoir. Thirty-Eighth Workshop on Geothermal Reservoir Engineering Stanford University, Stanford, California.

Lynne, B. Y., & Campbell, K. A. (2004). Morphologic and Mineralogic Transitions from Opal-A to Opal-CT in Low-Temperature Siliceous Sinter Diagenesis, Taupo Volcanic Zone, New Zealand. *Journal of Sedimentary Research*, 74(4), 561-579.

Lynne, B. Y., Campbell, K. A., James, B. J., Browne, P. R., & Moore, J. (2007). Tracking Crystallinity in Siliceous Hot-Spring Deposits. *American Journal of Science*, 307(3), 612-641.

Moore, D. M., & Reynolds Jr, R. C. (1989). X-Ray Diffraction and the Identification and Analysis of Clay Minerals. Oxford University Press (OUP).

Welton, J. E. (1984). SEM Petrology Atlas American Association of Petroleum Geologists Tulsa, OK.